Organic Electronics 13 (2012) 1365–1369

Contents lists available at SciVerse ScienceDirect

Organic Electronics

journal homepage: www.elsevier.com/locate/orgel

Air stable organic complementary inverter with high and balance noise margin based on polymer/metal oxide hybrid gate dielectrics

Ting-Hsiang Huang, Hsin-Cheng Lai, Bo-Jie Tzeng, Zingway Pei *

Graduate Institute of Optoelectronic Engineering, Department of Electrical Engineering, National Chung Hsing University, Taichung 402, Taiwan, ROC

ARTICLE INFO

Article history:
Received 5 December 2011
Received in revised form 23 March 2012
Accepted 1 April 2012
Available online 28 April 2012

Keywords:
Air-stable
Organic complementary inverter
Balanced noise margin

ABSTRACT

This study demonstrates an ambient air operated organic complementary inverter composed of a pentacene p-channel and a *N*,*N*′-ditridecylperylene-3,4,9,10-tetracarboxylic diimide n-channel organic thin-film transistor (TFT) fabricating at room temperature. The gate dielectric is an ultrathin polystyrene-co-methyl methacrylate (PS-r-PMMA)-modified hafnium oxide hybrid layer. Grafting the PS-r-PMMA passivates the surface defects. The transistors exhibit balanced performance, including threshold voltage, on/off current ratio, and field effect mobility. Similar channel dimensions for both types of TFT can be designed for the inverter construction. The inverter operates well below 6 V. The switching voltage is approximately $V_{dd}/2$ with a high noise margin (87% of theoretical value), which is suitable for flexible logic applications.

1. Introduction

Organic thin-film transistors (OTFTs) have attracted attention because of properties such as flexibility, low-temperature processing, and low cost. Most OTFT research has examined large area sensors [1,2], display backplanes [3,4], and logic circuits [5–7]. An inverter is a fundamental element when building an electrical function block for logic circuit and sensor applications. Fig. 1(a) shows a complementary inverter that consists of a p-channel OTFT and an n-channel OTFT with a logic symbol, where the gate between the two OTFTs connects the signal input. The p-channel OTFT source is connected to the supply voltage, the drain contacts of the p-channel and n-channel OTFT are connected to the output, and the n-channel OTFT source is connected to the ground. An inverter with a complementary structure consumes less power with less propagation time delay during operation, which is suitable for low-power electronics. To enhance the advantages of complementary inverters, balanced performance, such as mobility and threshold voltages for n and p-channel OTFTs, is preferred. The organic material for a p-channel OTFT is generally pentacene or a derivative because they exhibit high mobility ($\mu \sim 1\ cm^2/V\ s$) and air stability. The material for an n-channel OTFT is usually either C60 [6] or hexadecafluorocopperphthalocyanine ($F_{16}CuPc$) [7]. However, these materials either exhibit relatively low mobility or are unstable in air. The low mobility makes the area for the n-channel OTFTs quite larger than the p-channel OTFTs. The unstable device must be further encapsulated or operated in a N_2-filled environment. Recently, a *N*,*N*′-ditridecylperylene-3,4,9,10-tetracarboxylic diimide (PTCDI-C13) n-channel OTFT has been shown to exhibit high mobility comparable to the mobility of pentacene [8]. However, the field-effect mobility depends on the growth temperature. With a higher substrate temperature, using Al or Au as source and drain electrodes, PTCDI-C13 based OTFTs exhibit higher mobility. Mobility also depends on the choice of gate dielectric and on whether OTFTs are operated in air or in an inert ambient environment. Surface-modified dielectrics and post-annealing recently improved air stability [9,10].

* Corresponding author. Present address: Graduate Institute of Optoelectronic Engineering, Department of Electrical Engineering, National Chung Hsing University, 250, Kuo Kuang Rd., Taichung 40227, Taiwan, ROC. Tel.: +886 422851549; fax: +886 422851410.
E-mail address: zingway@dragon.nchu.edu.tw (Z. Pei).

1566-1199/$ - see front matter © 2012 Elsevier B.V. All rights reserved.
http://dx.doi.org/10.1016/j.orgel.2012.04.006

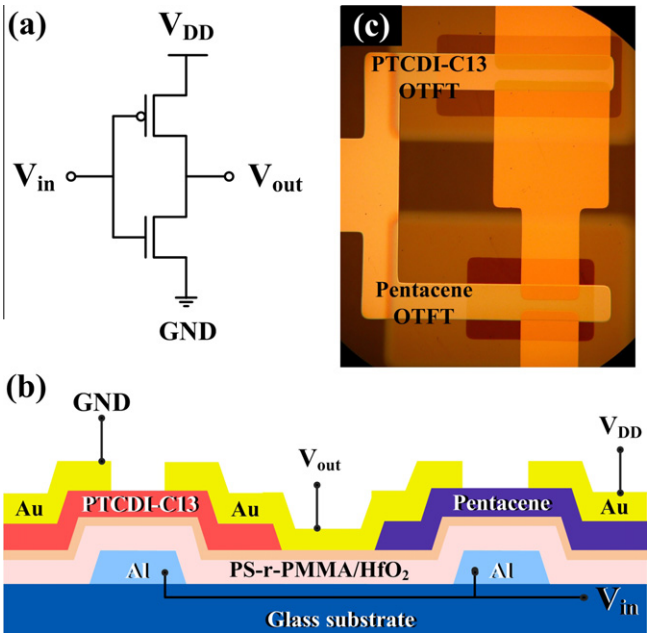

Fig. 1. (a) Circuit symbol of the complementary inverter. (b) OCTFT structure with PS-r-PMMA/HfO_x dielectrics. (c) Optical microscope image of OCTFT.

Tatemichi et al. [9] reported that PTCDI-C13 OTFTs with silicon dioxide as the gate dielectric exhibit an electron mobility of 2.1 cm^2/V s in a vacuum after 140 °C annealing. Without post-annealing, mobility is low at approximately 10^{-3} cm^2/V s. There is also no TFT behavior when operating in air. Jang et al. [10] reported that PTCDI-C13 OTFTs can have electron mobilities as large as 0.83 cm^2/V s in air by post-annealing at 120–140 °C and protecting the hydrophilic SiO_2 surface with a high T_g polymer. This research suggests that proper dielectric/semiconductor interfaces can improve the stability of PTCDI-C13. Post-annealing can increase field-effect mobility. Tanidaa et al. [11] showed that shallow level interface traps affect the field-effect mobility of PTCDI-C13 OTFTs. Applying a PMMA layer on SiO_2 suppresses these shallow level interface traps.

This study examines an organic complementary TFT (OCTFT) inverter consisting of room temperature-deposited PTCDI-C13 and pentacene for n- and p-channel OTFTs, respectively, with balanced performance and a high noise margin operating in the ambient air environment. For an OTFT, a low leakage, smooth, high capacitance, surface passivated dielectric is essential to maintain operation stability [12]. The hafnium oxide (HfO_x) with polystyrene-co-methyl methacrylate (PS-r-PMMA) modification layer was used as the gate dielectric. The high dielectric constant of HfO_x ($k \sim 15$) [13] kept the OTFT operating at low voltage with low leakage current. The ultrathin PS-r-PMMA smoothed the HfO_x surface and suppressed the channel carrier scattered by the hydroxyl group (OH^-) induced traps in the HfO_x *[13]. Such a structure provides stable organic semiconductor/dielectric interfaces, leading to balanced electrical performances for PTCDI-C13 and pentacene OTFTs.*

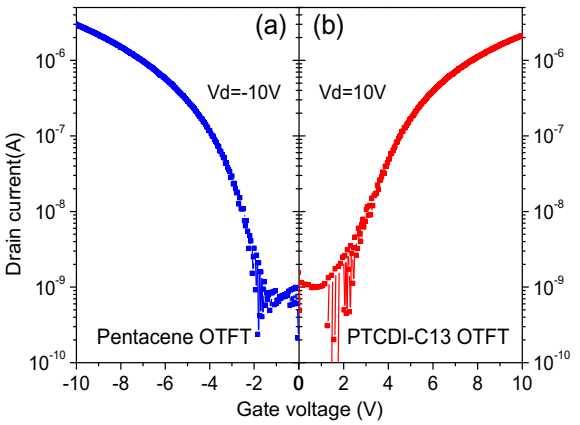

Fig. 2. Symmetry transfer curves of pentacene and PTCDI-C13 OTFTs.

2. Experiment

Fig. 1(b) shows the organic inverter with PS-r-PMMA/HfO_x dielectrics used in this study. An 80-nm-thick aluminum gate electrode was grown by thermal evaporation on the glass substrate. The 80-nm-thick HfO_x dielectric was deposited by RF sputtering at room temperature and then treated with oxygen plasma. The PS-r-PMMA (Aldrich, M_w = 100,000–150,000) dissolved in toluene (20 mg/ml) was spin-coated on the HfO_x and annealed on a hotplate at 170 °C for 12 h in a nitrogen atmosphere. This process enabled copolymer chains to diffuse and attach to the HfO_x. The unattached PS-r-PMMA chains were rinsed in toluene for 30 s to obtain an ultrathin PS-r-PMMA (approximately 10 nm). [14] The capacitance of 80-nm-thick HfO_x and surface PS-r-PMMA is approximately 166 nF/cm^2. [13] The

Table 1
Summary of OTFT performance.

Channel	W/L (μm)	V_{th} (V)	μ (cm^2/V s)	S.S (V/Dec.)	I_{on}/I_{off} (A)
Pentacene	500/100	−2.8	0.2	0.99	$10^{-6}/10^{-9}$
PTCDI-C13	1000/100	3	0.07	2.31	$10^{-6}/10^{-9}$

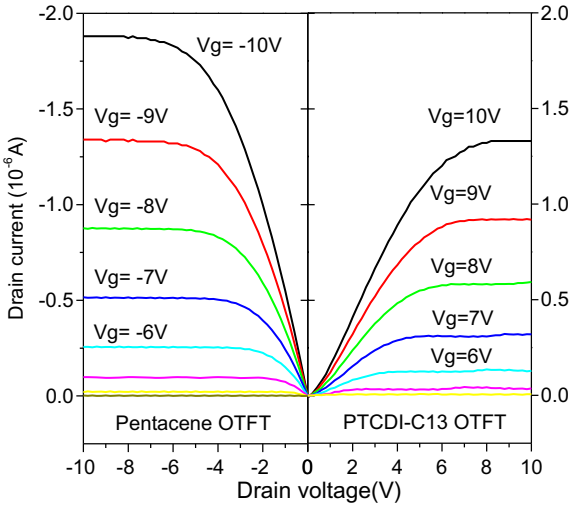

Fig. 3. Output curves of both type OTFTs with PS-r-PMMA/HfO_x.

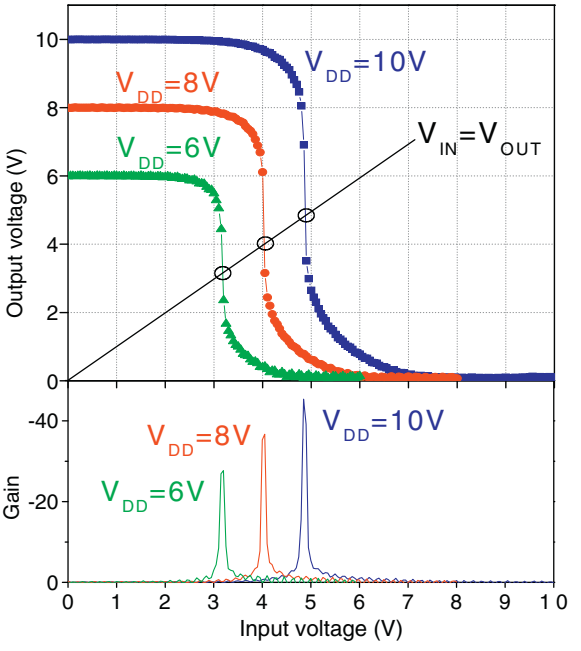

Fig. 4. Voltage transfer characteristic and corresponding gain of the organic inverter.

pentacene (Aldrich, 99%) and PTCDI-C13 (Aldrich, 95%) organic semiconductors (used as received) were evaporated in 40-nm-thick without substrate heating at a base pressure of 2×10^{-6} torr. The deposition rates for pentacene and PTCDI-C13 were 1 Å/s and 0.3 Å/s, respectively. Finally, gold electrodes were thermally evaporated to complete transistor source/drain contacts connecting the pentacene and PTCDI-C13 OTFTs. The patterning of the gate, semiconductors, and source/drain electrodes was accomplished by the evaporation of materials through corresponding metal shadow masks. Fig. 1(c) shows that the channel length (L) for both OTFTs was 100 μm. The channel widths (W) for the PTCDI-C13 and pentacene OTFTs were 1000 μm and 500 μm, respectively. The OTFT output and transfer curves and the inverter voltage transfer characteristic (VTC) were performed by an HP 4145A semiconductor analyzer. All electrical measurements were conducted in ambient air.

3. Results and discussion

Fig. 2(a) shows the transfer curves (I_d–V_g) of a p-channel pentacene OTFT with PS-r-PMMA/HfO_x dielectrics. The threshold voltage (V_{thp}), on/off current ratio (I_{on}/I_{off}), and subthreshold swing (S.S) are −2.8 V, 10^3, and, 0.99 V/dec, respectively. The field effect mobility extracted from the saturation region is approximately 0.2 cm^2/V s. The transfer curve of the n-channel PTCDI-C13 OTFT, as shown in Fig. 2(b), is symmetric to the pentacene OTFT. The field effect mobility in the saturation region and threshold voltage (V_{thn}) are approximately 0.07 cm^2/V s and 3 V, respectively, which is comparable to the pentacene OTFT results. The balanced performance of p- and n-channel OTFTs simplifies the circuit design. Table 1 lists the electrical parameters of both n and p-channel OTFTs. In addition to the balanced performance, both transistors operated in the enhancement mode, indicating that PS-r-PMMA provides suitable semiconductor/insulator interfaces for n- and p-channel organic semiconductors. The PS-r-PMMA layer screens the shallow level electron traps in the HfO_x. The charges attracted by gate voltage accumulate at the dielectric/semiconductor with little influence from these traps. However, because the HfO_x was grown at room temperature, the high density of pin-holes may not be fully passivated by the thin polymer modification layers [12]. The carriers might scatter at the pinholes. Therefore, mobility is not as high as the PTCDI-C13 OTFTs fabricated at an elevated temperature [8–11].

Fig. 3 shows the output curves of p-channel pentacene and n-channel PTCDI-C13 OTFTs with PS-r-PMMA/HfO_x dielectrics. Both output curves exhibit suitable transistor output behaviors. Applying a voltage of 0 to approximately 10 V shows the clear linear and saturation regions. With the increased drain voltage, the output current at saturation region almost unchanged for both types of transistor, indicates an high output impedance.

A logic circuit requires reliable complementary inverters with a sufficient static gain (dV_{OUT}/dV_{IN}) and noise margin (NM). Switching voltage (V_M) and the transition region

Table 2
Summary on inverter performance.

W_n/W_p	V_{DD} (V)	Maximum dV_{OUT}/dV_{IN}	NM_H (V)	NM_L (V)	ΔV_{IN} (V)	V_M (measured) (V)	V_M (estimated) (V)
1000/500	6	−27.7	2.05	2.8	1.25	3.16	3.11
	8	−36.7	3.05	3.45	1.5	4.04	4.20
	10	−45.4	4.4	4.35	1.15	4.87	5.29

Table 3
Comparison of inverter performance to other all organic complementary inverter.

Ref.	Dielectric	Channel	V_{th} (V)	μ (cm^2/V s)	V_{DD} (V)	V_M (V)	Gain (V/V)	NM (%)
[5]	SAM/AlO_x	N: F_{16}CuPC	<0.6	0.02	3	1.1	~100	–
		P: pentacene	<1.2	0.6				
[15]	SiO_2	N: F_{16}CuPC	2.5	0.005	2	0.9	15	33
		P: pentacene	−0.7	0.5				
[6]	Polystyrene/Al_2O_3	N: C_{60}	2.1	2.17	5	2.4	180	>80
		P: pentacene	−2.7	0.33				
[16]	HMDS/SiO_2/$TiSiO_2$/SiO_2	N:C_{60}	0.8	0.68	3	1.56	~120	–
		P: pentacene	−0.84	0.59				
[17]	Polyimide/SiO_2	N: PTCDI-C8	5.87	0.34	50	26	14	92.4
		P: pentacene	−12.9	0.92				
[18]	COC/SiO 2	N: PTCDI-C13	–	0.83	30	~20	45	–
		P: pentacene	–	1.56				
This work	PS-r-PMMA/HfO_x	N: PTCDI-C13	3	0.07	10	4.87	45.4	87
		P: pentacene	−2.8	0.2				

SAM: Self-assembled layer; HMDS: hexamethyldisilazane; PS-R-PMMA: poly (styrene-co-methyl methacrylate); COC: ethylene-norbornene cyclic olefin copolymers.

(ΔV_{IN}) between logic "0" and "1" dominate the NM. The $V_M = V_{DD}/2$ design is essential for an ideal inverter that produces high and balanced values noise margin values. By assuming the mobility and threshold voltages are constants, the switch voltage and current gain factor (β) are defined as the following equations:

$$\beta = \frac{\mu C_i W}{L} \tag{1}$$

$$V_M = \frac{\sqrt{\beta_n/\beta_p}V_{thn} + (V_{DD} - V_{thp})}{1 + \sqrt{\beta_n/\beta_p}} \tag{2}$$

in which μ is mobility, C_i is gate capacitance, β_n and β_p are n- and p-channel TFT current gain factors, and V_{thn} and V_{thp} are the n- and p-channel TFT threshold voltages. Because V_{thn} and V_{thp} are similar, to achieve $V_M = V_{DD}/2$ is easily by taking $\beta_n/\beta_p = 1$ with appropriate channel dimension (W/L) in device.

Accounting for the mobility of both TFTs, channel widths of $W_n = 1000$ μm and $W_p = 500$ μm were designed for the organic inverter. Fig. 4 shows organic inverter performance including the voltage transfers characteristics and corresponding static gains. The maximal gains of −36.7 V/V and −45.4 V/V were obtained at $V_{DD} = 8$ V and $V_{DD} = 10$ V, respectively. The measured switch voltages are approximately half of V_{DD}. Table 2 lists the inverter performance. From $V_{DD} = 6$ V to $V_{DD} = 10$ V, the difference between high noise margin (NM_H) and low noise margin (NM_L) is close. At $V_{DD} = 10$ V, a balanced noise margin is obtained, where the inverter shows an NM_H of 4.4 V and NM_L of 4.35 V. Additionally, the sharp transition region of approximately 1.15 V leads to the inverter with minimal power consumption. Such a high and equalized organic inverter NM exhibits 87% of the theoretical limitations. For switching voltage, the predicted V_M from (2) are only slightly different from the measurements. A V_M of approximately $V_{DD}/2$ is obtained.

Table 3 lists the comparison of the inverter performance with different dielectric and organic semiconductors [5,6,15–18]. In particular, compared to the organic complementary inverter with either F_{16}CuPc [5] or C60 [6] for N-type OTFTs, the inverter in this work exhibits all enhancement mode operated OTFTs, balanced threshold voltage and mobility, and a higher noise margin. Compared to the organic complementary inverter with the same PTCDI-based material [17,18] as the N-type OTFT, the proposed inverter operates at decreased voltage with higher gains without post-annealing.

4. Conclusions

This study demonstrates that polymer modified metal oxide is suitable as a gate dielectric for an air-stable organic complementary inverter. The PTCDI-C13 and pentacene were deposited at room temperature for n- and p-channel OTFFs, respectively. For the PS-r-PMMA/HfO_x bilayer dielectrics, the surface and bulk hydroxyl groups and defects were passivated leading to a balanced threshold voltage and mobility for n- and p-channel OTFTs. The switching voltage is designed to be approximately $V_{DD}/2$. The inverter based on this structure produces a high and balanced NM_H of 4.4 V and a NM_L of 4.35 V, which is 87% of the theoretical value. Additionally, there is an inverter gain of −45.4 V/V at 10 V.

Acknowledgements

The work was supported by National Science Council of Republic of China under grant NSC-99-2628-E-005-004. The authors thank Prof. Kou-Chen Liu from Electro-Optical Engineering, Chang Gung University for providing HfO_x samples.

References

[1] T. Someya, T. Sekitani, S. Iba, Y. Kato, H. Kawaguchi, T. Sakurai, A large-area, flexible pressure sensor matrix with organic field-effect transistors for artificial skin applications, Proc. Natl. Acad. Sci. USA 101 (2004) 9966–9970.
[2] T. Someya, Y. Kato, S. Iba, Y. Noguchi, T. Sekitani, H. Kawaguchi, T. Sakurai, Integration of organic FETs with organic photodiodes for a large area, flexible, and lightweight sheet image scanners, IEEE Trans. Electron Devices 52 (2005) 2502–2511.
[3] L. Zhou, S. Park, B. Bai, J. Sun, S.-C. Wu, T.N. Jackson, S. Nelson, D. Freeman, Y. Hong, Pentacene TFT driven AM OLED displays, IEEE Electron Device Lett. 26 (2005) 640–642.
[4] M. Mizukami, N. Hirohata, T. Iseki, K. Ohtawara, T. Tada, S. Yagyu, T. Abe, T. Suzuki, Y. Fujisaki, Y. Inoue, S. Tokito, T. Kurita, Flexible AM OLED panel driven by bottom-contact OTFTs, IEEE Electron Device Lett. 27 (2006) 249–251.
[5] H. Klauk, U. Zschieschang, J. Pflaum, M. Halik, Ultralow-power organic complementary circuits, Nature 445 (2007) 745–748.
[6] X.-H. Zhang, W.J. Potscavage, S. Choi, B. Kippelen, Low-voltage flexible organic complementary inverters with high noise margin and high dc gain, Appl. Phys. Lett. 94 (2009) 043312.
[7] T. Sekitani, U. Zschieschang, H. Klauk, T. Soyema, Flexible organic transistors and circuits with extreme bending stability, Nat. Mater. 9 (2010) 1015–1022.
[8] D.J. Gundlach, K.P. Pernstich, G. Wilckens, M. Grüter, S. Haas, High mobility n-channel organic thin-film transistors and complementary inverters, J. Appl. Phys. 98 (2005) 064502.
[9] S. Tatemichi, M. Ichikawa, T. Koyama, Y. Taniguchi, High mobility n-type thin-film transistors based on *N*,*N*′-ditridecyl perylene diimide with thermal treatments, Appl. Phys. Lett. 89 (2006) 112108.
[10] J. Jang, S. Nam, D.S. Chung, S.H. Kim, W.M. Yun, C.E. Park, High T_g cyclic olefin copolymer gate dielectrics for *N*,*N*′-ditridecyl perylene diimide based field-effect transistors: improving performance and stability with thermal treatment, Adv. Funct. Mater. 20 (2010) 2611–2618.
[11] S. Tanidaa, K. Nodaa, H. Kawabatab, K. Matsushigea, Investigation of electron trapping behavior in n-channel organic thin-film transistors with ultrathin polymer passivation on SiO_2 gate insulator, Synth. Metals 160 (2010) 1574–1578.
[12] T.-H. Huang, Z. Pei, W.-K. Lin, S.-T. Chang, K.-C. Liu, Oligomer semiconductor/dielectric interface modification for organic thin film transistor hysteresis reduction, Thin Solid Films 518 (2010) 7381–7384.
[13] T.-H. Huang, K.-C. Liu, Z. Pei, W.-K. Lin, S.-T. Chang, A poly(styrene-co-methyl methacrylate)/room-temperature sputtered hafnium oxide bi-layer dielectrics as gate insulator for a low voltage organic thin-film transistors, Org. Electron. 12 (2011) 1527–1532.
[14] T.-H. Huang, H.-C. Huang, Z. Pei, Temperature-dependent ultra-thin polymer layer for low voltage organic thin-film transistors, Org. Electron. 11 (2010) 618–625.
[15] S.D. Vusser, S. Steudel, K. Myny, J. Genoe, P. Heremans, Low voltage complementary organic inverters, Appl. Phys. Lett. 88 (2006) 162116.
[16] M. Kitamura, Y. Arakawa, Low-voltage-operating complementary inverters with C60 and pentacene transistors on glass substrates, Appl. Phys. Lett. 91 (2007) 053505.
[17] W.-Y. Chou, B.-L. Yeh, H.-L. Cheng, B.-Y. Sun, Y.-C. Cheng, Y.-S. Lin, S.-J. Liu, F.-C. Tang, C.-C. Chang, Organic complementary inverters with polyimide films as the surface modification of dielectrics, Org. Electron. 10 (2009) 1001–1005.
[18] J. Jang, S. Nam, D.S. Chung, S.H. Kim, W.M. Yun, C.E. Park, High T_g cyclic olefi n copolymer gate dielectrics for *N*′,*N*′-ditridecyl perylene diimide based field-effect transistors: improving performance and stability with thermal treatment, Adv. Funct. Mater. 20 (2010) 2611–2618.